Sound Field Reproduction Using Planar and Linear Arrays of Loudspeakers

Jens Ahrens and Sascha Spors

***Abstract*—In this paper, we consider physical reproduction of sound fields via planar and linear distributions of secondary sources (i.e., loudspeakers). The presented approach employs a formulation of the reproduction equation in spatial frequency domain which is explicitly solved for the secondary source driving signals. Wave field synthesis (WFS), the alternative formulation, can be shown to be equivalent under equal assumptions. Unlike the WFS formulation, the presented approach does not employ a far-field approximation when linear secondary source distributions are considered but provides exact results. We focus on the investigation of the spatial truncation and discretization of the secondary source distribution occurring in real-world implementations and present a rigorous analysis of evanescent and propagating components in the reproduced sound field.**

***Index Terms*—Ambisonics, spatial aliasing, spectral division method, wave field synthesis, spatial Fourier transform.**

I. Introduction

TWO alternative groups of approaches targeting the physical recreation of sound fields have evolved. The first group of these approaches bases on the straightforward solution of the reproduction equation for the loudspeaker driving signals. The best-known representative of these approaches is Ambisonics. Its initial formulation is presented in [1]. The alternative is known as wave field synthesis (WFS), e.g., [2], and is derived from the Rayleigh integrals and from the Kirchhoff–Helmholtz integral [3] respectively.

A number of approaches closely related to Ambisonics have been presented, e.g., [4]–[10]. The loudspeaker driving signals are determined via a formulation of the reproduction equation in the spherical harmonics domain which leads to an equation system which is solved. Alternatively, the approach presented in [11] straightforwardly sets up a simultaneous equation system. Approaches [4]–[7], [11] employ numerical algorithms in the solution of the equation system and are therefore computationally expensive and give only little insight into the fundamental properties of the actual reproduced sound field. The analytical formulations presented in [8]–[10], however, are perfectly transparent and therefore overcome above mentioned shortcomings.

Manuscript received February 19, 2009; revised November 18, 2009. Date of publication February 02, 2010; date of current version October 15, 2010. The associate editor coordinating the review of this manuscript and approving it for publication was Dr. Michael L. Seltzer.

The authors are with the Quality and Usability Lab, Deutsche Telekom Laboratories, Technische Universität Berlin, 10587 Berlin, Germany (e-mail: jens.ahrens@telekom.de; sascha.spors@telekom.de).

Digital Object Identifier 10.1109/TASL.2010.2041106

Approaches [5], [6], [8], [9] cannot be applied on linear and planar secondary source[1] contours but are restricted to circular and spherical ones. Approach [10] on the other hand is generally applicable on arbitrary enclosing loudspeaker arrangements but has been explicitly applied only on spherical ones. Such a restriction does finally not hold for [4], [7], [11]. However, the formulation of the latter does not exploit any *a priori* knowledge of the actual loudspeaker setup giving away the potential to reduce computational complexity and does not exhibit the transparency of analytical approaches. We therefore seek for alternative solutions.

WFS, the alternative to the above mentioned approaches, e.g., [2] and [12], employs a modified formulation of the Kirchhoff–Helmholtz integral to determine the loudspeaker driving signals in an analytical and efficient manner. In the case of planar and linear setups of omnidirectional loudspeakers, the resulting formulation is equivalent to Rayleigh's first integral formula [3]. However, the resulting formulation allows for a loudspeaker directivity compensation only within the limits of the stationary phase approximation which is applied in the approach [13].

In the context of WFS, the process of compensating for deviations of the properties of the reproduction system from the theoretical requirements (e.g., freefield conditions or omnidirectional secondary sources) is typically formulated on the basis of the theory of multiple-input-multiple-output (MIMO) systems, e.g., [14]–[17]. The compensation is thus not included in the fundamental physical formulation.

The adaptation of the Ambisonics-like analytical approach from [8] to the employment of planar and linear loudspeaker arrangements has already been presented by the authors in [18]. The reproduction equation is formulated in the spatial frequency domain (in this case it is the wavenumber domain) in order to analytically derive the secondary source driving signals. Due to the fact that for any given geometry the secondary source driving signals are always yielded by a division in a suitable spatial spectrum domain, we term the approach *spectral division method* (SDM).

In this paper, we revisit the formulation of the SDM from [18] and concentrate on the investigation of the consequences of spatial discretization and truncation occurring in real-world implementations. The SDM is principally not restricted to the employment of secondary monopole sources. However, we focus on the fundamental physical properties of the approach and do not explicitly treat complex secondary sources.

[1]We do not speak of loudspeakers but rather of *secondary sources* in the context of continuous distributions. The term secondary source represents a more abstract concept of a spatially continuous sound source than the notion of loudspeakers which typically refers to something discrete.

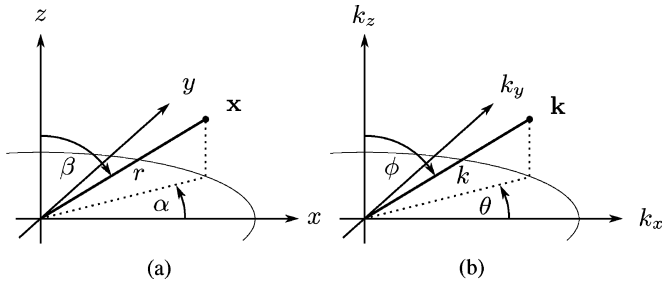

Fig. 1. Coordinate systems used in this paper. (a) Spatial domain. (b) Wavenumber domain.

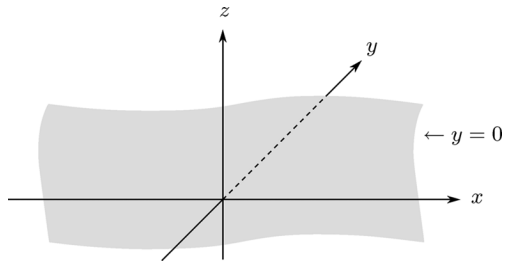

Fig. 2. Illustration of the setup of a planar secondary source situated along the x-z-plane. The secondary source distribution is indicated by the gray shading and has infinite extent. The target half-space is the half-space bounded by the secondary source distribution and containing the positive y-axis.

Nomenclature: The following notational conventions are used. For scalar variables, lowercase denotes the time domain, uppercase the temporal frequency domain. The spatial frequency domain (wavenumber domain) is indicated by a tilde over the respective symbol. The dependent variables of a given quantity in the spatial frequency domain indicate with respect to which dimension the spatial frequency domain is considered, e.g., $\tilde{P}(k_x, y, z, \omega)$ means that $P(\mathbf{x}, \omega)$ is considered in the wavenumber domain only with respect to k_x.

Vectors are denoted by lowercase boldface. The three-dimensional position vector in Cartesian coordinates is given as $\mathbf{x} = [x\ y\ z]^T$. Refer also to the coordinate systems depicted in Fig. 1.

The acoustic wavenumber is denoted by k. It is related to the temporal frequency by $k^2 = (\omega/c)^2$ with ω being the radial frequency and c the speed of sound.

Outgoing spherical waves are denoted by $(1/|\mathbf{x}|)e^{-jk|\mathbf{x}|}$, monochromatic plane waves by $e^{-j\mathbf{k}_{\mathrm{pw}}^T\mathbf{x}}$, with $\mathbf{k}_{\mathrm{pw}}^T = [k_{\mathrm{pw},x}\ k_{\mathrm{pw},y}\ k_{\mathrm{pw},z}] = k_{\mathrm{pw}} \cdot [\cos\theta_{\mathrm{pw}} \sin\phi_{\mathrm{pw}}\ \sin\theta_{\mathrm{pw}} \sin\phi_{\mathrm{pw}}\ \cos\phi_{\mathrm{pw}}]$ and $(\theta_{\mathrm{pw}}, \phi_{\mathrm{pw}})$ being the propagation direction of the plane wave. j is the imaginary unit ($j = \sqrt{-1}$).

We refer to secondary sources rather than to loudspeakers since we assume their distributions to be continuous at first stage.

II. Derivation of the Secondary Source Driving Functions

In order to analyze the properties of the sound field reproduced by planar and linear secondary source distributions, we have to find the appropriate secondary source driving signals. The procedure is outlined in the following.

In each subsection, we exemplarily derive the explicit driving signals to reproduce a sample plane wave of given propagation direction and frequency. The obtained results can be straightforwardly extended to the reproduction of complex sound fields via the *angular spectrum representation* [3]. The latter represents the decomposition of wave fields into a continuum of plane waves in a source-free region. The appropriate combination of the driving signals for plane waves as indicated by the angular spectrum representation yields the driving signals for a given complex sound field to be reproduced.

For simplicity, we assume the secondary sources to be omnidirectional since this is the simplest and most revealing case.

A. Continuous Planar Secondary Source Arrays

The sound field reproduced by secondary sources continuously distributed along the x-z-plane (refer to Fig. 2) is given by [18]

$$P(\mathbf{x}, \omega) = \iint_{-\infty}^{\infty} D(\mathbf{x}_0, \omega) \cdot G(\mathbf{x} - \mathbf{x}_0, \omega)\, dx_0 dz_0 \qquad (1)$$

where $\mathbf{x}_0 = [x_0\ 0\ z_0]^T$ denotes the position of the secondary source driven by the signal $D(\mathbf{x}_0, \omega)$. $G(\mathbf{x} - \mathbf{x}_0, \omega)$ denotes the spatio-temporal transfer function of the secondary source located at $\mathbf{x}_0$, i.e., the temporal spectrum of the sound field it emits when it is fed by a temporal impulse. Note that we assume $G(\,\cdot\,)$ to be shift invariant (we write $G(\mathbf{x} - \mathbf{x}_0, \omega)$ instead of $G(\mathbf{x}|\mathbf{x}_0, \omega)$) [3]. This requires that all secondary sources have to have equal spatio-temporal characteristics and orientation.

Before solving (1) for the secondary source driving signal, we have to note that we cannot expect to be able to reproduce arbitrary sound fields. The given secondary source setup will only be capable of creating wave fronts that propagate away from it. Furthermore, the secondary source distribution divides the space into two half-spaces one of which we have to choose as target half-space in which we reproduce the desired sound field. The reproduced sound field in the other half-space is a byproduct whose properties are determined by the secondary source driving function $D(\mathbf{x}_0, \omega)$ and the directivity of the secondary sources in that half-space.

We consider these constraints by choosing the half-space bounded by the x-z-plane (the secondary source distribution) and containing the positive y-axis as the target half-space. We furthermore allow only wave fronts traveling into the target half-space to be reproduced.

In order to simplify the mathematical treatment, we replace the positional coordinate y in all considered quantities with $|y|$ and indicate the replacement by subscripting a given position dependent quantity with $|y|$, e.g., $G_{|y|}(x, y, z) = G(x, |y|, z)$. Such a function $G_{|y|}$ then exhibits the property $G_{|y|}(x, y, z) = G_{|y|}(x, -y, z) = G_{|y|}(x, |y|, z)$. This has the following consequences. 1) All considered quantities are symmetric with respect to the secondary source distribution. 2) We loose all information about the half-space containing the negative y-axis. Consequence 2) is not a drawback since, as we have noted above, only one half-space can be controlled independently anyway.

Equation (1) essentially constitutes a two-dimensional convolution along the spatial dimensions x and z, respectively. This fact is revealed when (1) is rewritten as

$$\begin{aligned} P(\mathbf{x},\omega) &= \iint_{-\infty}^{\infty} D([x_0\ 0\ z_0]^T,\omega) \\ &\quad \times G([x\ y\ z]^T - [x_0\ 0\ z_0]^T,\omega)\, dx_0 dz_0 \\ &= \iint_{-\infty}^{\infty} D(x_0,0,z_0,\omega) \\ &\quad \times G(x-x_0,y,z-z_0,\omega)\, dx_0 dz_0 \\ &= D(\mathbf{x}|_{y=0},\omega) *_x *_z G(\mathbf{x},\omega) \end{aligned} \tag{2}$$

where the asterisk $*_i$ denotes convolution with respect to the indexed spatial dimension [19]. Thus, the convolution theorem

$$\tilde{P}_{|y|}(k_x,y,k_z,\omega) = \tilde{D}(k_x,k_z,\omega)\cdot \tilde{G}_{|y|}(k_x,y,k_z,\omega) \tag{3}$$

holds [19]. Refer to Appendix A for the definition of the Fourier transform used in this paper.

The secondary source driving function in wavenumber domain is given by

$$\tilde{D}(k_x,k_z,\omega) = \frac{\tilde{P}_{|y|}(k_x,y,k_z,\omega)}{\tilde{G}_{|y|}(k_x,y,k_z,\omega)} \tag{4}$$

and in temporal spectrum domain by

$$\begin{aligned} D(x,z,\omega) = \frac{1}{4\pi^2} \iint_{-\infty}^{\infty} &\frac{\tilde{P}_{|y|}(k_x,y,k_z,\omega)}{\tilde{G}_{|y|}(k_x,y,k_z,\omega)} \\ &\times e^{-jk_x x} e^{-jk_z z}\, dk_x dk_z. \end{aligned} \tag{5}$$

In order that $\tilde{D}(k_x,k_z,\omega)$ and $D(x,z,\omega)$ are defined $\tilde{G}_{|y|}(k_x,y,k_z,\omega)$ may not exhibit zeros.

From (4) and (5) it is obvious that the driving signal is essentially yielded by a division in spatial frequency domain. We therefore refer to the presented approach as *spectral division method* (SDM). Equation (5) suggests that $D(x,z,\omega)$ is dependent on the distance y of the receiver to the secondary source distribution since y is apparent on the right-hand side of (5). It will be shown below that under certain circumstances, y does indeed cancel out making $D(x,z,\omega)$ independent from the location of the receiver.

Example: In the remainder of this subsection, we demonstrate the derivation of the driving function for a sample plane wave of given propagation direction to be reproduced by a continuous planar distribution of secondary point sources.

The explicit expressions for $\tilde{P}_{|y|}(k_x,y,k_z,\omega)$ and $\tilde{G}_{|y|}(k_x,y,k_z,\omega)$ are derived in the Appendices and are given by (49) and (53). Due to the constrained validity of the involved transformations, the following equations are only valid for $k_{\mathrm{pw},y} > 0$ (refer also to the appendices), i.e., for plane waves propagating into the target half-space.

The wavenumber domain representation of in (53) reveals that the spatio-temporal transfer function of omnidirectional sources do indeed have a propagating and an evanescent component. It is remarkable that choosing a propagating plane wave as desired sound field triggers exclusively the propagating part of $G_{|y|}(\cdot)$. Mathematically, this fact is reflected by the sifting property of the Dirac delta functions (49) which perfectly suppresses the evanescent component of $G_{|y|}(\cdot)$.

Inserting (49) and (53) into (4) and exploiting the sifting property of the delta function [19] yields

$$\begin{aligned} \tilde{D}_{\mathrm{pw}}(k_x,k_z,\omega) &= 8\pi^2 j k_{\mathrm{pw},y} \\ &\quad \cdot\delta(k_x - k_{\mathrm{pw},x})\,\delta(k_z - k_{\mathrm{pw},z}) \times 2\pi\delta(\omega-\omega_{\mathrm{pw}}). \end{aligned} \tag{6}$$

Note that $\tilde{D}_{\mathrm{pw}}(k_x,k_z,\omega)$ is indeed independent from y under the given assumptions.

Finally, the driving function is given by

$$D_{\mathrm{pw}}(x,z,\omega) = 2jk_{\mathrm{pw},y}\cdot e^{-jk_{\mathrm{pw},x}x}\, e^{-jk_{\mathrm{pw},z}z} \times 2\pi\delta(\omega-\omega_{\mathrm{pw}}). \tag{7}$$

Transferred to the time domain and formulated for broadband signals, (7) reads

$$\begin{aligned} d_{\mathrm{pw}}(x,z,t) &= \frac{2}{c}\sin\theta_{\mathrm{pw}}\sin\phi_{\mathrm{pw}} \\ &\quad \times \frac{\partial}{\partial t}\hat{s}\left(t - \frac{x}{c}\cos\theta_{\mathrm{pw}}\sin\phi_{\mathrm{pw}} - \frac{z}{c}\cos\phi_{\mathrm{pw}}\right) \end{aligned} \tag{8}$$

where $\hat{s}(t)$ denotes the time-domain signal that the plane wave carries. Thus, the driving signal for a secondary source at a given location is yielded by differentiating the time domain input signal with respect to time and weighting and delaying it. The differentiation and the weight are independent from the position of the secondary sources and can therefore be performed on the input signal. The delay is dependent both on the propagation direction of the desired plane wave as well as on the position of the secondary source. It therefore has to be performed individually for each secondary source. This constitutes a computationally efficient implementation scheme compared to the numerical approaches in [4], [7], [11]. The implementation scheme of the presented approach is similar to that of WFS [12] (refer also to Section IV).

Finally, note that the temporal derivation in (8) compensates for the spatial integration taking place in (1).

B. Continuous Linear Secondary Source Arrays

Despite the simple driving function for the planar secondary source array, this setup will be rarely implemented due to the enormous amount of loudspeakers necessary. Typically, audio reproduction systems employ linear arrays or a combination thereof. For convenience, the secondary source array is assumed to be along the x-axis (thus $\mathbf{x}_0 = [x_0\ 0\ 0]^T$, refer to Fig. 3).

For this setup the analog to the reproduction equation for planar arrays (1) is given by [18]

$$P_{|y|}(\mathbf{x},\omega) = \int_{-\infty}^{\infty} D(\mathbf{x}_0,\omega)\cdot G_{|y|}(\mathbf{x}-\mathbf{x}_0,\omega)\, dx_0. \tag{9}$$

Similarly to (1), (9) can be viewed as a convolution integral. In this case, the convolution is performed along the x-axis and the convolution theorem

$$\tilde{P}_{|y|}(k_x,y,z,\omega) = \tilde{D}(k_x,\omega)\cdot \tilde{G}_{|y|}(k_x,y,z,\omega) \tag{10}$$

holds. The secondary source driving function in wavenumber domain is thus given by

$$\tilde{D}(k_x,\omega) = \frac{\tilde{P}_{|y|}(k_x,y,z,\omega)}{\tilde{G}_{|y|}(k_x,y,z,\omega)} \tag{11}$$

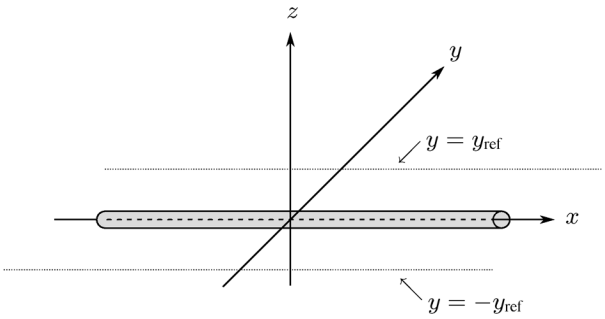

Fig. 3. Illustration of the setup of a linear secondary source situated along the x-axis. The secondary source distribution is indicated by the gray shading and has infinite extend. The target half-plane is the half-plane bounded by the secondary source distribution and containing the positive y-axis. Thin dotted lines indicate the reference lines (see text).

and in temporal spectrum domain by

$$D(x,\omega) = \frac{1}{2\pi} \int_{-\infty}^{\infty} \frac{\tilde{P}_{|y|}(k_x, y, z, \omega)}{\tilde{G}_{|y|}(k_x, y, z, \omega)} \, e^{-jk_x x} \, dk_x. \tag{12}$$

Again, $\tilde{G}_{|y|}(k_x, y, z, \omega)$ may not exhibit zeros.

As with planar secondary source distributions, we intentionally assumed $D(x,\omega)$ to be exclusively dependent on x because x is the only degree of freedom in the position of the secondary sources. See below for a discussion of the dependency of $D(x,\omega)$ on y and z.

Example: $\tilde{P}_{|y|}(k_x, y, z, \omega)$ and $\tilde{G}_{|y|}(k_x, y, z, \omega)$ for a plane wave and secondary monopole sources are given by (48) and (52).

Inserting (48) and (52) into (11) and applying the sifting property of the Dirac delta function yields

$$\tilde{D}_{\text{pw}}(k_x,\omega) = \frac{2\pi\delta(k_x - k_{\text{pw},x}) e^{-jk_{\text{pw},y}|y|} e^{-jk_{\text{pw},z} z}}{-\frac{j}{4} H_0^{(2)}\left(\sqrt{\left(\frac{\omega_{\text{pw}}}{c}\right)^2 - {k_{\text{pw},x}}^2}\sqrt{|y|^2 + z^2}\right)} \times 2\pi\delta(\omega - \omega_{\text{pw}}). \tag{13}$$

We find that $|y|$ and z are apparent in the expression for the driving function (13) suggesting that (9) can only be satisfied for positions on the surface of a cylinder determined by $d = \sqrt{|y|^2 + z^2}$.

However, with such a linear secondary source distribution like the one under consideration, the k_x, k_y and k_z components of the reproduced sound field cannot be controlled individually [3]. The secondary source distribution radiates conical wave fronts which have only one degree of freedom. The term $(\omega_{\text{pw}}/c)^2 - k_{\text{pw},x}^2$ in (13) is constant for a given temporal frequency ω_{pw} and given $k_{\text{pw},x}$ and the relations

$$\left(\frac{\omega_{\text{pw}}}{c}\right)^2 - k_{\text{pw},x}^2 = k_{\text{pw},y}^2 + k_{\text{pw},z}^2 \tag{14}$$

$$= \underbrace{k_{\text{pw}}^2(\sin^2\theta_{\text{pw}} \sin^2\phi_{\text{pw}} + \cos^2\phi_{\text{pw}})}_{=k_{\text{pw},\rho}^2}$$

$$= \text{const} \tag{15}$$

hold due to the dispersion relation. In order to illustrate (14) and (15) we temporarily switch to cylindrical coordinates. We assume the linear axis of the coordinate system to coincide with the secondary source distribution. $k_{\text{pw},\rho}$ denotes the radial wavenumber.

Relation (15) states that the radial wavenumber $k_{\text{pw},\rho}$ is solely dependent on the temporal frequency and the $k_{\text{pw},x}$ component of the virtual plane wave. For a given azimuth θ_{pw} of the propagation direction of the desired virtual plane wave, the zenith angle ϕ_{pw} is determined by relations (14) and (15) and vice versa.

In other words, when a correct propagation direction of the reproduced virtual plane wave is desired, (9) can only be satisfied for receiver positions on a straight line parallel to the secondary source distribution. On the opposite side of the secondary source distribution the reproduced sound field is also correct on an according line but its propagation direction is mirrored. In spherical coordinates, these two receiver lines are determined by $d = \sqrt{|y|^2 + z^2}$ and $(\alpha = \theta_{\text{pw}}, \beta = \phi_{\text{pw}})$ or $(\alpha = -\theta_{\text{pw}}, \beta = \pi - \phi_{\text{pw}})$. This finding is in analogy to the reproduction of a plane wave by a circular arrangement of secondary point sources where the reproduced sound field has to be referenced to a point [8]. As a consequence, a correct propagation direction of the reproduced sound field can only be achieved inside a target half-plane containing the secondary source distribution and the reference line.

We choose the horizontal plane containing the positive y-axis as target half-plane where we also assume the receiver (e.g., the listener's ears), thus $z \stackrel{!}{=} 0$. We consequently also have to limit the propagation directions of the desired plane wave to the horizontal plane ($\phi_{\text{pw}} \stackrel{!}{=} (\pi/2)$ or $k_{\text{pw},z} \stackrel{!}{=} 0$). We set $|y|$ to the desired distance $y_{\text{ref}} > 0$ from the secondary source array where we want the sound field to be correct. Note that (13) provides the potential to compensate for artifacts in listening positions off the target plane. However, due to the conical property of the reproduced sound field discussed above, phase errors and incorrect propagation directions of the reproduced sound field arise off the target plane. As will be explained more in detail in Section IV.B, this type of reproduction is typically referred to as 2(1/2)-dimensional reproduction.

With the above mentioned referencing, (13) simplifies to

$$\tilde{D}_{\text{pw}}(k_x,\omega) = \frac{4j \cdot e^{-jk_{\text{pw},y} y_{\text{ref}}}}{H_0^{(2)}(k_{\text{pw},y} y_{\text{ref}})} \cdot 2\pi\delta(k_x - k_{\text{pw},x}) \times 2\pi\delta(\omega - \omega_{\text{pw}}) \tag{16}$$

and finally

$$D_{\text{pw}}(x,\omega) = \frac{4j \cdot e^{-jk_{\text{pw},y} y_{\text{ref}}}}{H_0^{(2)}(k_{\text{pw},y} y_{\text{ref}})} \cdot e^{-jk_{\text{pw},x} x} \times 2\pi\delta(\omega - \omega_{\text{pw}}). \tag{17}$$

Transferred to the time domain and formulated for broadband signals, (17) reads

$$d_{\text{pw}}(x,t) = f(t) *_t \hat{s} \times \left(t - \frac{x}{c}\cos\theta_{\text{pw}} \sin\phi_{\text{pw}} - \frac{y_{\text{ref}}}{c} \sin\theta_{\text{pw}} \sin\phi_{\text{pw}}\right). \tag{18}$$

$f(t)$ denotes a filter with frequency response

$$F(\omega) = \frac{4j}{H_0^{(2)}(k_{\text{pw},y} y_{\text{ref}})}$$

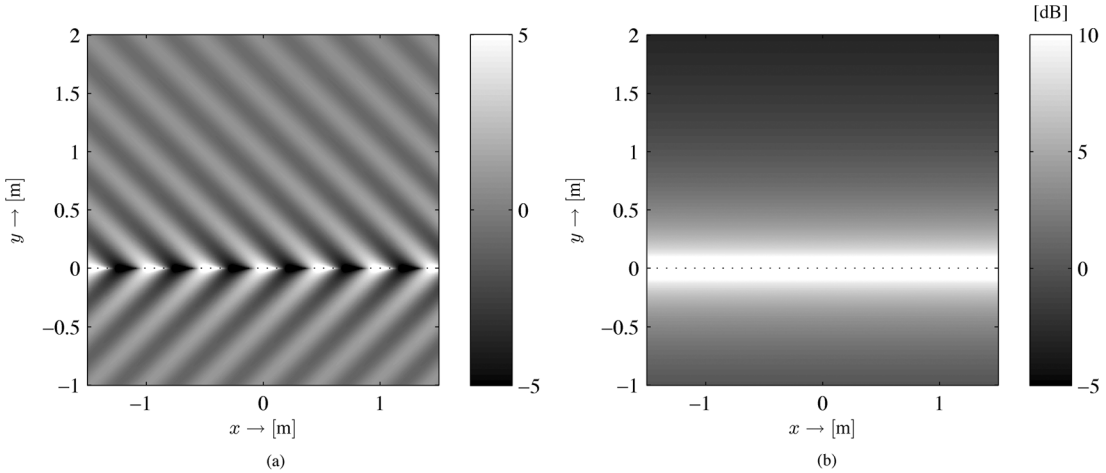

Fig. 4. Sound pressure $P_{\mathrm{pw},|\mathrm{y}|}(\mathbf{x},\omega)$ of a continuous linear distribution of secondary point sources reproducing a virtual plane wave of $f_{\mathrm{pw}} = 1000$ Hz and unit amplitude with propagation direction $\theta_{\mathrm{pw}} = (\pi/4)$ referenced to the distance $y_{\mathrm{ref}} = 1.0$ m. The secondary source distribution is indicated by the dotted line. Only the horizontal plane is shown. The values are clipped as indicated by the color bars. (a) $\Re\{P_{\mathrm{pw},|\mathrm{y}|}(\mathbf{x},\omega)\}$, (b) $20 \cdot \log_{10} |P_{\mathrm{pw},|\mathrm{y}|}(\mathbf{x},\omega)|$.

the asterisk $*_t$ denotes convolution with respect to time, and $\hat{s}(t)$ the time-domain signal that the plane wave carries. Thus, the time domain driving signal for a secondary source at a given location is yielded by applying a delay and a filter on the time domain input signal. The transfer function $F(\omega)$ of the filter has high-pass characteristics with a slope of approximately 3 dB per octave.

$F(\omega)$ is exclusively dependent on the propagation direction of the desired plane wave and on the amplitude reference distance y_{ref}. It is therefore equal for all secondary sources and it is sufficient to perform the filtering only once on the input signal before distributing the signal to the secondary sources. The delay is dependent both on the propagation direction of the desired plane wave and on the position of the secondary source. It therefore has to be performed individually for each secondary source.

As with planar secondary source distributions, this constitutes a computationally efficient implementation scheme compared to the numerical approaches in [4], [7], [11].

III. Reproduced Sound Fields

A. Planar Secondary Source Arrays

The sound field reproduced by a continuous planar secondary monopole distribution driven according to (7) is yielded by inserting (7) into (1). To solve the integrals one has to substitute $u = x_0 - x$ and $v = z_0 - z$ and follow the procedure outlined in Appendix C. One arrives then at (47) proofing perfect reproduction of the sample plane wave in the target half-space.

B. Linear Secondary Source Arrays

Inserting (17) into (9) yields the sound field reproduced by a continuous linear secondary monopole source distribution driven to reproduce the sample plane wave. Solving the integral as indicated in Section III-A yields

$$P_{\mathrm{pw},|\mathrm{y}|}(\mathbf{x},\omega) = \frac{e^{-jk_{\mathrm{pw},y}y_{\mathrm{ref}}}}{H_0^{(2)}(k_{\mathrm{pw},y}y_{\mathrm{ref}})} \times e^{-jk_{\mathrm{pw},x}x} H_0^{(2)}(k_{\mathrm{pw},y}\sqrt{|y|^2+z^2}). \quad (19)$$

For $|y| = y_{\mathrm{ref}}$ and $z = 0$ (19) exactly corresponds to the desired sound field. However, for $|y| \neq y_{\mathrm{ref}}$ or $z \neq 0$ the reproduced sound field differs from the desired one. The arising artifacts are easily identified when the far-field/high-frequency region is considered ($k_{\mathrm{pw},y}y_{\mathrm{ref}} \gg 1,\ k_{\mathrm{pw},y}\sqrt{|y|^2+z^2} \gg 1$). There, the Hankel functions appearing in (19) can be replaced by their large argument approximation $H_\nu^{(2)}(z) = \sqrt{2/\pi z}e^{-j(z-\nu(\pi)/2-(\pi/4))}$ [3]. The approximated reproduced sound field reads then

$$P_{\mathrm{appr,pw},|\mathrm{y}|}(\mathbf{x},\omega) = \sqrt{\frac{y_{\mathrm{ref}}}{\sqrt{|y|^2+z^2}}} \times e^{-jk_{\mathrm{pw},x}x} e^{-jk_{\mathrm{pw},y}\sqrt{|y|^2+z^2}}. \quad (20)$$

In the horizontal plane (the target plane, $z = 0$) in the far-field/high-frequency region, the amplitude of the reproduced sound field $P(\mathbf{x},\omega)$ shows a decay proportional to $\sqrt{|y|}^{-1}$, i.e., approximately 3 dB with each doubling of the distance to the secondary source array. In the near-field/low-frequency region the amplitude decay is slightly different and additionally, some subtle spectral deviations are apparent. These findings have also been derived by the authors in [8] for the reproduction of a plane wave with a circular secondary point source distribution. Refer also to Fig. 4. It depicts the real part and the magnitude of the sound pressure of a continuous linear distribution of secondary point sources reproducing a virtual plane wave of $f_{\mathrm{pw}} = 1000$ Hz and unit amplitude with propagation direction $\theta_{\mathrm{pw}} = (\pi/4)$ referenced to the distance $y_{\mathrm{ref}} = 1.0$ m.

The exact formulation of the driving function, (17), allows for referencing also in the proximity of the secondary source array. Thorough investigation of this procedure is beyond the scope of this paper and is subject to ongoing research.

IV. Comparison to the Rayleigh Formulation

In this section, we compare the presented approach to the alternative formulation given by the Rayleigh integrals [3]. For simplicity we exemplarily consider Rayleigh's first integral formula. The Rayleigh I integral states that a planar distribution

of secondary monopole sources is capable of reproducing a desired source-free sound field in one of the half-spaces bounded by the secondary source distribution. The sound field in the other half-space is a mirrored copy of the desired sound field.

Sound field reproduction based on Rayleigh's first integral equation is typically referred to as wave field synthesis (WFS) [2], [12].

The original formulation of WFS assumes that the secondary sources have monopole characteristics. As mentioned in Section I, a number of approaches have been proposed in order to compensate for loudspeaker characteristics which depart from this assumption. However, we limit the investigation to the fundamental formulations both of the presented approach as well as WFS. The approach and nomenclature used below follow [12].

A. Planar Secondary Source Distributions

Although we are not aware of the existence of a three-dimensional implementation of WFS we treat it theoretically for completeness.

For planar secondary source arrays in the x-z-plane the Rayleigh I integral [3]

$$P(\mathbf{x},\omega) = \iint_{-\infty}^{\infty} \underbrace{-2\frac{\partial}{\partial \mathbf{n}} S(\mathbf{x}|_{\mathbf{x}=\mathbf{x}_0},\omega)}_{=D_{\mathrm{WFS,3D}}(\mathbf{x}_0,\omega)} G_{\mathrm{3D}}(\mathbf{x}-\mathbf{x}_0,\omega)\, dx_0 dz_0 \tag{21}$$

states that the sound pressure in the half-spaces defined by the secondary source array is determined by an integration over all secondary sources driven by the driving signals $D_{\mathrm{WFS,3D}}(\mathbf{x}_0,\omega)$. The driving signals $D_{\mathrm{WFS,3D}}(\mathbf{x}_0,\omega)$ are given as the directional gradient $(\partial/\partial\mathbf{n})$ normal to the secondary source distribution of the desired sound field, whereby the normal points into the target half-space. As in Section II, we assume the half-space in positive y-direction to be the target area. Thus, the normal vector $\mathbf{n}$ is parallel to the y-axis. Note that the free-field Green's function $G_{\mathrm{3D}}(\mathbf{x}-\mathbf{x}_0,\omega)$ apparent in (21) essentially represents the monopole sources employed in Section II [3].

Deriving the driving function for a monochromatic plane wave with temporal angular frequency ω_{pw} propagating into the direction $(\theta_{\mathrm{pw}},\phi_{\mathrm{pw}})$ as indicated in (21) yields

$$D_{\mathrm{WFS,3D}}(\mathbf{x},\omega) = 2jk_{\mathrm{pw},y}\cdot e^{-j\mathbf{k}_{\mathrm{pw}}^T\mathbf{x}}\cdot 2\pi\delta(\omega-\omega_{\mathrm{pw}}). \tag{22}$$

$D_{\mathrm{WFS,3D}}(\mathbf{x},\omega)$ evaluated at $y=0$ essentially corresponds to the driving function of the presented approach given by (7), thus proofing the equivalence of the two approaches when planar distributions of secondary monopole sources are employed.

B. Linear Secondary Source Distributions

To apply the Rayleigh I integral (21) on linear secondary source distributions we have to claim that the reproduced sound field is independent from the z-coordinate. The setup can then be reinterpreted as a linear distribution of secondary line sources parallel to the z-axis positioned along the x-axis. The WFS formulation then reads [12]

$$P(\mathbf{x},\omega) = \int_{-\infty}^{\infty} \underbrace{-2\frac{\partial}{\partial \mathbf{n}} S(\mathbf{x}|_{\mathbf{x}=\mathbf{x}_0},\omega)}_{=D_{\mathrm{WFS,2D}}(\mathbf{x}_0,\omega)} G_{\mathrm{2D}}(\mathbf{x}-\mathbf{x}_0,\omega)\, dx_0. \tag{23}$$

The driving function for a monochromatic plane wave with angular frequency ω_{pw} propagating into the direction $(\theta_{\mathrm{pw}},(\pi/2))$ evaluated at $y=0, z=0$ is then

$$D_{\mathrm{WFS,2D}}(x,\omega) = 2jk_{\mathrm{pw},y}\cdot e^{-jk_{\mathrm{pw},x}x}\cdot 2\pi\delta(\omega-\omega_{\mathrm{pw}}). \tag{24}$$

The two-dimensional WFS (23) employs the two-dimensional free-field Green's function [3]

$$G_{\mathrm{2D}}(\mathbf{x}-\mathbf{x}_0,\omega) = \frac{j}{4}H_0^{(2)}\left(\frac{\omega}{c}|\mathbf{x}-\mathbf{x}_0|\right) \tag{25}$$

which can be interpreted as the spatial transfer function of a line source. However, WFS typically employs loudspeakers with closed cabinets as secondary sources whose behavior is better approximated by that of point sources. This secondary source mismatch has to be compensated for.

In the far-field/high-frequency region $G_{\mathrm{2D}}(\mathbf{x}-\mathbf{x}_0,\omega)$ can be approximated as (refer to Section III-B)

$$G_{\mathrm{2D}}(\mathbf{x}-\mathbf{x}_0,\omega) \approx \sqrt{\frac{2\pi}{j\frac{\omega}{c}}}\sqrt{|\mathbf{x}-\mathbf{x}_0|}\cdot \underbrace{\frac{1}{4\pi}\frac{e^{-j\frac{\omega}{c}|\mathbf{x}-\mathbf{x}_0|}}{|\mathbf{x}-\mathbf{x}_0|}}_{=G_{\mathrm{3D}}(\mathbf{x}-\mathbf{x}_0,\omega)} \tag{26}$$

where the spatial transfer function $G_{\mathrm{3D}}(\mathbf{x}-\mathbf{x}_0,\omega)$ of a point source is apparent [refer to (51)]. This employment of secondary sources suitable for three-dimensional reproduction in two-dimensional reproduction is typically referred to as 2(1/2)-dimensional reproduction [12], [13], [20], [21].

In the far-field/high-frequency region the secondary source mismatch can be compensated for as [12]

$$D_{\mathrm{appr,WFS,2.5D}}(x,\omega) = \sqrt{\frac{2\pi}{jk_{\mathrm{pw}}}}\sqrt{y_{\mathrm{ref}}}\cdot D_{\mathrm{WFS,2D}}(x,\omega) \tag{27}$$

with y_{ref} denoting the reference distance. More explicitly,

$$D_{\mathrm{appr,WFS,2.5D}}(x,\omega) = \sqrt{8\pi y_{\mathrm{ref}}}\sqrt{jk_{\mathrm{pw}}}\sin\theta_{\mathrm{pw}} \times e^{-jk_{\mathrm{pw},x}x}\cdot 2\pi\delta(\omega-\omega_{\mathrm{pw}}). \tag{28}$$

The far-field/high-frequency approximation of the driving function of the presented approach (17) reads

$$D_{\mathrm{appr,2.5D}}(x,\omega) = \sqrt{8\pi y_{\mathrm{ref}}}\sqrt{jk_{\mathrm{pw}}}\sqrt{\sin\theta_{\mathrm{pw}}} \times e^{-jk_{\mathrm{pw},x}x}\cdot 2\pi\delta(\omega-\omega_{\mathrm{pw}}). \tag{29}$$

As a consequence of the fact that the driving functions of the two approaches differ by an amplitude factor, the reproduced sound fields differ as well by the same factor.

The reproduced sound fields can only be compared in the far-field/high-frequency region because the WFS driving function only holds there. It can indeed be shown that

$$P_{\mathrm{WFS,pw,|y|}}(\mathbf{x},\omega) = \sqrt{\sin\theta_{\mathrm{pw}}}\cdot\ P_{\mathrm{appr,pw,|y|}}(\mathbf{x},\omega). \quad (30)$$

where $P_{\mathrm{appr,pw,|y|}}(\mathbf{x},\omega)$ is given by (20). From (19) and (20), it can be seen that the presented approach provides the desired result and a sound field which coincides with the desired one on the receiver line. We therefore have to conclude that the standard WFS driving function (28) has to be corrected by a factor of $\sqrt{\sin\theta_{\mathrm{pw}}}$ in order to perform comparably to the presented approach in the far-field/high-frequency region.

The source of error in WFS seams to lie in the far-field/high-frequency approximation in (26). In the traditional WFS formulation like [13], [20], and [21], the stationary phase approximation is applied which can be shown to yield the same results like the approximation performed in (26). These two approaches of referencing have therefore to be considered being equivalent.

From (26) it becomes clear that the reproduced sound field in WFS is actually not referenced to a line but to a circle around the individual secondary sources. The apparent consequence is the incorrect amplitude when $\sqrt{\sin\theta_{\mathrm{pw}}} \neq 1$. This amplitude deviation is low for $\sqrt{\sin\theta_{\mathrm{pw}}} \approx 1$ but can reach several dB for $\sqrt{\sin\theta_{\mathrm{pw}}}$ deviating strongly from 1, i.e., for virtual plane wave fronts which are not approximately parallel to the secondary source distribution.

Due to the general equivalence of the Rayleigh formulation and the present approach under the given assumptions as shown above, the driving function for a given desired sound field to be reproduced may be calculated either via the directional gradient [the Rayleigh formulation, (21) and (23)] or via the spatial Fourier transform [the presented approach, (5) and (12)] depending on which approach is considered more convenient.

V. Comparison to the Ambisonics Formulation

As stated in Section I, Ambisonics constitutes the alternative to WFS sound field reproduction. Modern formulations such as [6], and [8]–[10] assume a continuous secondary source distribution enclosing the receiver area. The reproduction equation is then given by

$$P(\mathbf{x},\omega) = \int_{S_0} D(\mathbf{x}_0,\omega)\, G(\mathbf{x}-\mathbf{x}_0)\, d\mathbf{x}_0 \quad (31)$$

where S_0 describes the secondary source contour, i.e., $\mathbf{x}_0 \in S_0$.

Equation (31) is explicitly solved in a transformed domain. The basis functions of the latter are dependent on the geometry of the secondary source contour, e.g., spherical harmonics are employed for spherical secondary source distribution. In this transformed domain, mode-matching is applied in order to yield the individual spatial modes of the driving function $D(\mathbf{x}_0,\omega)$.

The approach presented in this paper actually follows the same procedure like the Ambisonics approaches outlined above [compare (31) to (1) and (9)]. The presented approach can therefore be considered as an extension of Ambisonics to planar and linear secondary source distributions.

The fundamental difference is the fact that the infinite extension of the secondary source distribution assumed in the presented approach leads to a continuous spatial spectrum. An enclosing secondary source distribution as it is employed in the Ambisonics context constitutes a finite domain and therefore leads to discrete spectra [19]. Since the spatial spectra employed in the presented approach are continuous, a discrete mode-matching can not be applied but has to be performed in a continuous manner. Refer to (4) and (13).

An Ambisonics-like encoding of the desired sound field into a finite number of discrete spatial modes which represent a bandlimited subset of the system's eigenfunctions cannot be accomplished.

VI. Discretization of the Secondary Source Distribution

So far, we have assumed the secondary source distributions to be continuous. However, practical implementations of sound field reproduction systems will always employ spatially discrete loudspeakers. The consequences of this spatial discretization are investigated in this section on the example of a virtual plane wave reproduced by distributions of secondary point sources.

The procedure employed in this section is an extension of [21] and [22]. We investigate the spatial properties of the reproduced sound field for a given temporal frequency ω. An alternative approach examining the properties of the reproduced sound field over the entire temporal frequency range with respect to the wavenumber along one spatial dimension can be found in [23].

A. Planar Secondary Source Distributions

We consider an infinite planar secondary source array of constant spacing between adjacent secondary sources (loudspeakers) of Δx and Δz in x-and z-direction, respectively. We model the spatial discretization by sampling the driving function as [22]

$$D_S(x,z,\omega) = \frac{1}{\Delta x}\sum_{\eta=-\infty}^{\infty}\delta(x-\Delta x\eta) \cdot\frac{1}{\Delta z}\sum_{\nu=-\infty}^{\infty}\delta(z-\Delta z\nu)\times D(x,z,\omega). \quad (32)$$

It can be shown that $\tilde{D}_S(k_x,k_z,\omega)$ is then

$$\tilde{D}_S(k_x,k_z,\omega) = \sum_{\eta=-\infty}^{\infty}\sum_{\nu=-\infty}^{\infty}\tilde{D}\left(k_x-\frac{2\pi}{\Delta x}\eta, k_z-\frac{2\pi}{\Delta z}\nu,\omega\right). \quad (33)$$

For the virtual plane wave considered in this section, the sound field $P_{S,|y|}(\mathbf{x},\omega)$ reproduced by such an array is yielded by inserting (6), (33), and (53) into (3) and applying an inverse Fourier transform. $P_{S,|y|}(\mathbf{x},\omega)$ is given by

$$\begin{aligned} P_{S,|y|}(\mathbf{x},\omega) &= 2jk_{\mathrm{pw,y}}\cdot\sum_{\eta=-\infty}^{\infty}\sum_{\nu=-\infty}^{\infty} \\ &\quad\times\tilde{G}_{|y|}\left(\frac{2\pi}{\Delta x}\eta+k_{\mathrm{pw,x}},\ y,\ \frac{2\pi}{\Delta z}\nu+k_{\mathrm{pw,z}},\ \omega\right) \\ &\quad\times e^{-j\left(\frac{2\pi}{\Delta x}\eta+k_{\mathrm{pw,x}}\right)x}e^{-j\left(\frac{2\pi}{\Delta z}\nu+k_{\mathrm{pw,z}}\right)z} \\ &\quad\cdot\ 2\pi\delta(\omega-\omega_{\mathrm{pw}}). \end{aligned} \quad (34)$$

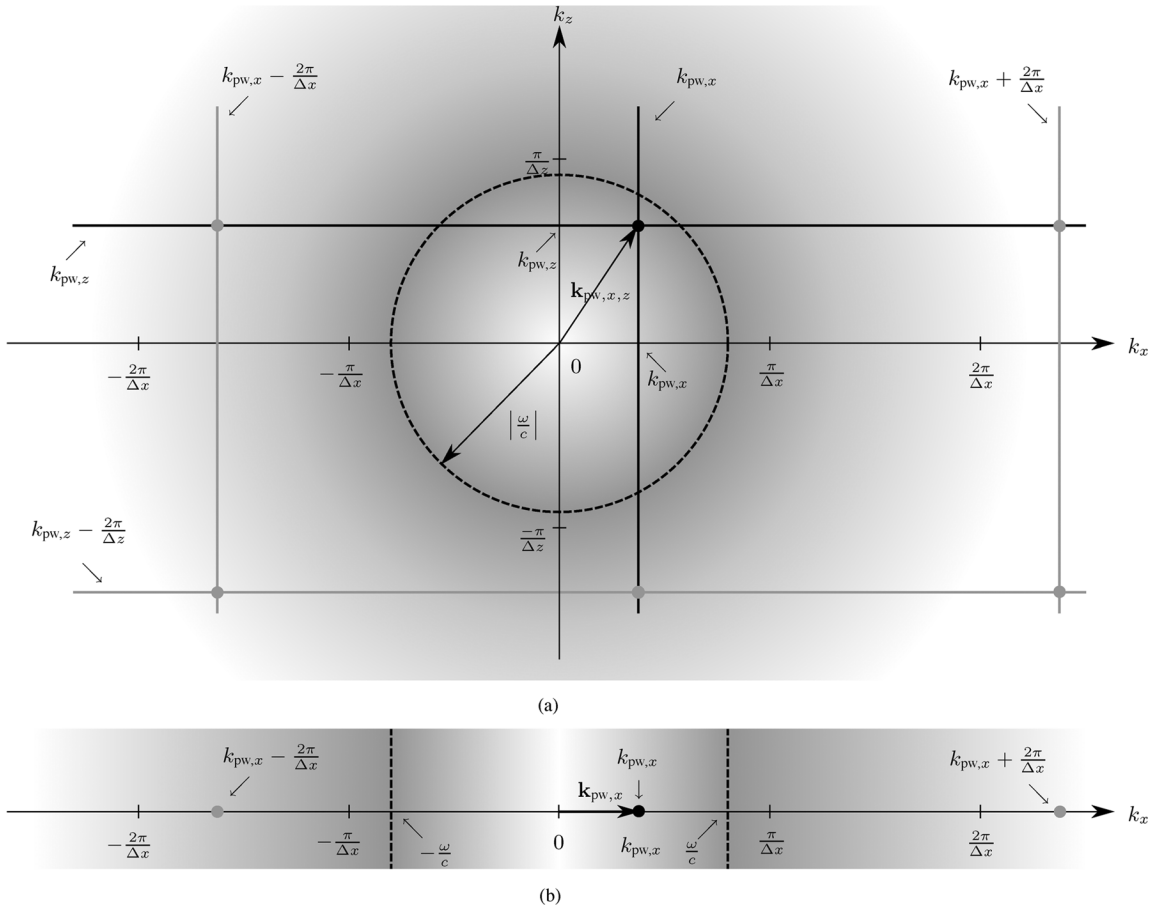

Fig. 5. Illustration of the consequences of the discretization of the secondary source distributions for planar distributions [Fig. 5(a)] and linear distributions [Fig. 5(b)] by means of illustrating $\tilde{G}_{|y|}(\,\cdot\,)$. The dots • indicate reproduced components. Black solid lines and black dots represent quantities occurring with continuous secondary source distributions. Gray lines and dots represent quantities occurring additionally due to the spatial discretization. The gray shading indicates the amplitude of $\tilde{G}_{|y|}(\,\cdot\,)$. (a) Illustration of $\tilde{G}_{|y|}(k_x, y, k_z, \omega)$ reflecting the properties of discrete planar secondary source distributions [(34)]. The vector $\mathbf{k}_{\mathrm{pw},x,z} = [k_{\mathrm{pw},x}\ k_{\mathrm{pw},z}]^T$ represents the propagation direction of the virtual plane wave projected onto the k_x-k_z-plane. The dots • indicate reproduced components. Locations outside the circle represent evanescent sound fields, locations inside the circle represent propagating sound fields. (b) Illustration of $\tilde{G}_{|y|}(k_x, y, z, \omega)$ reflecting the properties of discrete linear secondary source distributions [(37)]. The vector $\mathbf{k}_{\mathrm{pw},x} = [k_{\mathrm{pw},x}]$ represents the propagation direction of the virtual plane wave projected onto the k_x-axis. Locations outside the interval $[-(\omega/c); (\omega/c)]$ represent evanescent sound fields, locations inside represent propagating sound fields.

$P_{S,|y|}(\mathbf{x}, \omega)$ is thus given by a summation over a multiplication of three factors. The latter describe the reproduced sound field along each individual dimension of space. Equation (34) evaluated for $(\eta = 0, \nu = 0)$ constitutes the desired plane wave. The other terms in the sum for $\eta \neq 0$ and $\nu \neq 0$ are aliasing contributions.

For each individual order η and ν, the reproduced sound field in x- and z-direction is given by complex exponential functions. The amplitude is therefore constant along the respective dimension and the phase changes harmonically. The reproduced sound field along the y-dimension is determined by the secondary source transfer function $\tilde{G}_{|y|}(k_x, y, k_z, \omega)$ given by (53). Since $\tilde{G}_{|y|}(k_x, y, k_z, \omega)$ essentially determines the properties of $P_{S,|y|}(\mathbf{x}, \omega)$, we limit the investigation to the properties of the former.

Fig. 5(a) illustrates $\tilde{G}_{|y|}(k_x, y, k_z, \omega)$ in the k_x-k_z-plane. For a fixed temporal frequency ω, $k_x = (2\pi/\Delta x)\eta + k_{\mathrm{pw,x}}$ is represented by straight lines perpendicular to the k_z-axis. $k_z = (2\pi/\Delta z)\nu + k_{\mathrm{pw},z}$ is represented by straight lines perpendicular to the k_x-axis. $\tilde{G}_{|y|}(k_x, y, k_z, \omega)$ has a pole on a circular region of radius (ω/c) centered around the origin of the coordinate system.

Reproduced components of $P_{S,|y|}(\mathbf{x}, \omega)$ are given by the intersections of the above described lines in the k_x-k_z-plane. The desired plane wave is indicated in Fig. 5(a) by the intersection of the two lines inside the circle of radius $|(\omega/c)|$.

Two categories of aliasing artifacts can be identified. 1) Evanescent[2] components and 2) additional propagating plane wave components. Artifacts belonging to category 1) are illustrated in Fig. 5(a). They are represented by intersections of lines occurring at locations where $\sqrt{k_x^2 + k_z^2} > |(\omega/c)|$. It can be seen from (53) that $P_{S,|y|}(\mathbf{x}, \omega)$ is evanescent for exactly these locations. Note that the exponent in (53) is purely real for $\sqrt{k_x^2 + k_z^2} > |(\omega/c)|$. The existence of evanescent components in the reproduced sound field has already been indicated in [23].

Since neither η nor ν is bounded, these evanescent aliasing artifacts cannot be avoided. Due to the monotonically decreasing

[2]A sound field which decays with respect to a given direction and does not experience any phase alteration along this direction is termed *evanescent* in this paper.

amplitude of $\tilde{G}_{|y|}(k_x, y, k_z, \omega)$ [indicated by the gray shading in Fig. 5(a)] for $\sqrt{k_x^2 + k_z^2} > |(\omega/c)|$, the higher the orders η and ν of the aliasing contributions are, the lower are their amplitudes.

The aliasing artifacts of category 2) occur only in special situations. When the distance Δx or Δz between adjacent loudspeakers is so large, respectively, if the temporal frequency ω is so high that lines other than those for $(\eta = 0, \nu = 0)$ intersect inside the circular region bounded by the pole of $\tilde{G}_{|y|}(k_x, y, k_z, \omega)$. In this case, the aliasing artifacts are additional plane wave contributions whose propagation direction is determined by the location of the points of intersection and is therefore dependent on the temporal frequency ω. Note that this situation is not apparent in Fig. 5(a). For ease of clarity $\Delta x, \Delta z$, and ω in Fig. 5(a) where chosen such that the lines for $\eta \neq 0$ and $\nu \neq 0$ only intersect outside the circular boundary between the regions of propagating and evanescent components.

It is not straightforward to derive a revealing analytical anti-aliasing condition for planar secondary source distributions which prevents the reproduction of unwanted propagating components. This is due to the fact that the sampling in x-dimension and the sampling in z-dimension interact and cannot be treated independently. We therefore leave the reader with the conditions

$$\left(\frac{\omega}{c}\right)^2 < \left(\frac{2\pi}{\Delta x} - |k_{pw,x}|\right)^2 + k_{pw,z}^2 \tag{35}$$

$$\left(\frac{\omega}{c}\right)^2 < k_{pw,x}^2 + \left(\frac{2\pi}{\Delta z} - |k_{pw,z}|\right)^2 \tag{36}$$

which both have to be met.

Note that typical implementations of sound field reproduction methods use loudspeaker spacings of several centimeters. This results in propagating aliasing artifacts above a few thousand Hertz. Recall that the audible frequency range significantly exceeds 15 kHz. As a consequence, reproduced sound fields are heavily corrupted by spatial aliasing. There are indications that the human ear is not very sensitive towards this type of artifacts when stationary situations are considered. Results obtained in the context of wave field synthesis for stationary scenarios show that spatial aliasing artifacts are perceived as a rather subtle though audible timbral coloration [24] and can impair localization with respect to various properties including accuracy and apparent source width [21], [25], [26].

B. Linear Secondary Source Distributions

Applying the procedure outlined in Section VI-A on linear secondary source distributions leads to the sound field $P_{S,|y|}(\mathbf{x}, \omega)$ reproduced by a discrete linear secondary source distribution reading

$$P_{S,|y|}(\mathbf{x}, \omega) = \frac{8j\pi e^{-jk_{\mathrm{pw},y} y_{\mathrm{ref}}}}{H_0^{(2)}(k_{\mathrm{pw},y} y_{\mathrm{ref}})} \sum_{\eta=-\infty}^{\infty} e^{-j\left(\frac{2\pi}{\Delta x}\eta + k_{\mathrm{pw,x}}\right)x} \times \tilde{G}_{|y|}\left(\frac{2\pi}{\Delta x}\eta + k_{\mathrm{pw,x}},\ y,\ z,\ \omega\right) \cdot 2\pi\delta(\omega - \omega_{\mathrm{pw}}). \tag{37}$$

Again, $P_{S,|y|}(\mathbf{x}, \omega)$ is given by a complex exponential function along the x-dimension. The properties of the secondary sources reflected in $\tilde{G}_{|y|}(k_x, y, z, \omega)$ given by (52) determine $P_{S,|y|}(\mathbf{x}, \omega)$ in radial direction, i.e., along $\sqrt{y^2 + z^2}$.

The situation for discrete linear secondary source distributions is very similar to that of discrete planar distributions discussed in Section VI-A: The considered region of the wavenumber space, in this case the k_x-axis, is divided into regions implying different properties of the reproduced sound field. 1) Locations where $k_x < |(\omega/c)|$ represent a combination of propagating and evanescent sound fields, 2) locations where $k_x > |(\omega/c)|$ represent purely evanescent sound fields.

This finding is deduced from the properties of the secondary source transfer function $\tilde{G}_{|y|}(k_x, y, z, \omega)$. For $k_x < |(\omega/c)|$, $\tilde{G}_{|y|}(k_x, y, z, \omega)$ is given by the zeroth order Hankel function of second kind $H_0^{(2)}(\cdot)$ (refer to (52)). This indicates a combination of a propagating and an evanescent sound field [3]. For $k_x > |(\omega/c)|$, $\tilde{G}_{|y|}(k_x, y, z, \omega)$ is given by the zeroth order modified Bessel function of second kind $K_0(\cdot)$. $K_0(\cdot)$ is purely real and decreases strictly monotonically with increasing argument, i.e., with increasing distance $\sqrt{y^2 + z^2}$ to the secondary source distribution (refer to Footnote 2).

The locations $k_x = (2\pi/\Delta x)\eta + k_{\mathrm{pw,x}}$ in (37) are represented by black dots in Fig. 5(b). Locations where $k_x < |(\omega/c)|$ represent the reproduction of the combination of a propagating and an evanescent sound field as described by the Hankel function. Locations where $k_x > |(\omega/c)|$ indicate the reproduction of a purely evanescent component. As with planar secondary source distributions, the purely evanescent components cannot be avoided since η is not bounded. Again, higher orders η lead to lower amplitudes of the aliasing contributions in the purely evanescent region $k_x > |(\omega/c)|$.

If only $\eta = 0$ falls into the region where $k_x < |(\omega/c)|$, the reproduced propagating sound field consists exclusively of the desired sound field plus an according evanescent component. This situation is illustrated in Fig. 5(b). Note that all reproduced propagating components are accompanied by an additional evanescent component as described by the Hankel function in (52).

However, if the spacing Δx between adjacent secondary sources is big enough, respectively, if the temporal angular frequency ω is chosen high enough, then also reproduced components for $\eta \neq 0$ fall into the region where $k_x < |(\omega/c)|$. In this case, propagating spatial aliasing artifacts arise which are accompanied by an according evanescent component as discussed above. This situation is not illustrated in Fig. 5(b). These propagating spatial aliasing artifacts constitute additional plane waves. The according location inside the region where $k_x < |(\omega/c)|$ determines the k_x-component of the propagation direction of the additional plane wave fronts. Note that the propagation directions of the additional plane wave fronts are dependent on the temporal frequency ω. This finding has been derived in [27] for purely two-dimensional reproduction.

The anti-aliasing condition preventing undesired propagating aliasing contributions can be graphically deduced from Fig. 5(b). It reads

$$\omega < \frac{2\pi c}{\Delta x(1 + |\cos\theta_{\mathrm{pw}}|)}. \tag{38}$$

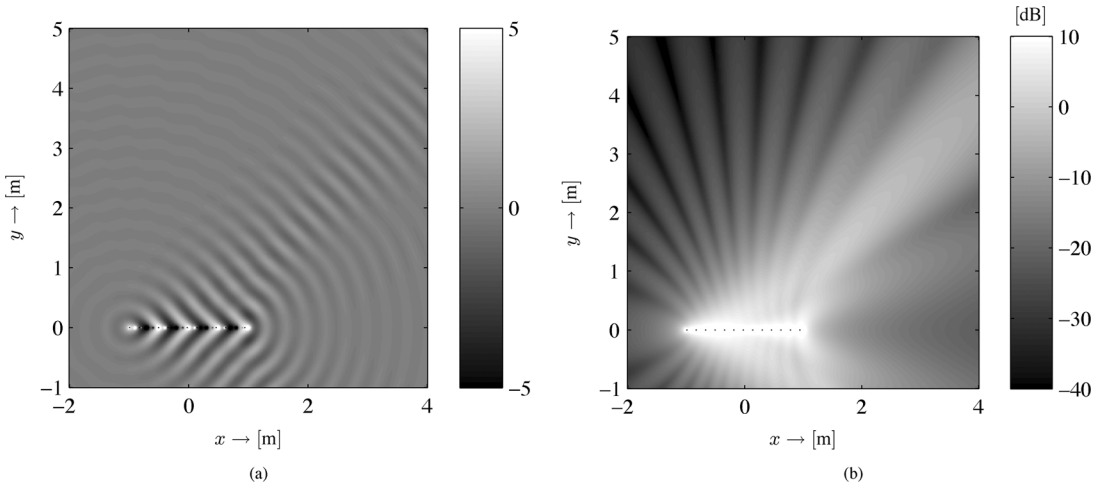

Fig. 6. Sound pressure $P_{\mathrm{S,tr,pw}}(\mathbf{x},\omega)$ of a discrete linear distribution of secondary point sources reproducing a virtual plane wave of $f_{\mathrm{pw}} = 1000$ Hz and unit amplitude with propagation direction $\theta_{\mathrm{pw}} = (\pi/4)$ referenced to the distance $y_{\mathrm{ref}} = 1.0$ m. The secondary source distribution is indicated by the dotted line. $\Delta x = 0.1$ m, $L = 2$ m. The values are clipped as indicated by the color bars. (a) $\Re\{P_{\mathrm{S,tr,pw}}(\mathbf{x},\omega)\}$, (b) $20 \cdot \log_{10} |P_{\mathrm{S,tr,pw}}(\mathbf{x},\omega)|$.

Equation (38) has already been derived in [22] for purely two-dimensional reproduction and in [20], [21], [23] for 2(1/2)-dimensional reproduction.

VII. Truncation of the Secondary Source Distribution

Practical implementations of sound field reproduction systems will always be of finite length. The consequences of this spatial truncation are treated in this section. For convenience, we explicitly consider a continuous linear secondary source distribution which is truncated in x-dimension. We then comment on how to extend the findings to planar secondary source distributions.

The spatial truncation is modeled by multiplying the secondary source driving function $D(\mathbf{x}_0,\omega)$ with a suitable window function $w(x_0)$ [21]. Incorporating $w(x_0)$ into (9) yields the sound field $P_{\mathrm{tr},|y|}(\mathbf{x},\omega)$ of a truncated planar source distribution as

$$P_{\mathrm{tr},|y|}(\mathbf{x},\omega) = \int_{-\infty}^{\infty} w(x_0) D(\mathbf{x}_0,\omega)\, G(\mathbf{x}-\mathbf{x}_0,\omega)\, dx_0. \tag{39}$$

The convolution theorem (10) then reads [19]

$$\tilde{P}_{\mathrm{tr},|y|}(k_x,y,z,\omega) = \frac{1}{2\pi} \underbrace{(\tilde{w}(k_x) *_{k_x} \tilde{D}(k_x,\omega))}_{=\tilde{D}_{tr}(k_x,\omega)} \times \tilde{G}_{|y|}(k_x,y,z,\omega) \tag{40}$$

where the asterisk $*_{k_x}$ denotes convolution with respect to the spatial frequency variable k_x.

The finite extent of a secondary source distribution of length L centered around $x = 0$ can be modeled by a rectangular window $w_R(x)$ as

$$w_R(x) = \mathrm{rect}\left(\frac{x}{L}\right) = \begin{cases} 1, & \text{for} |x| \le \frac{L}{2} \\ 0, & \text{elsewhere.} \end{cases} \tag{41}$$

The Fourier transformation of $w_R(x)$ with respect to x is [3]

$$\tilde{w}_R(k_x) = L \cdot \frac{\sin\frac{k_x L}{2}}{\frac{k_x L}{2}} = L \cdot \mathrm{sinc}\left(\frac{k_x L}{2\pi}\right). \tag{42}$$

For the interpretation of (40) we consider again the reproduction of a plane wave. Recall $\tilde{D}(k_x,\omega)$ given by (16). The convolution of $\tilde{D}(k_x,\omega)$ with $\tilde{w}_R(k_x)$ is essentially a spatial low pass filtering operation smearing $\tilde{D}(k_x,\omega)$ along the k_x-axis. The Dirac $\delta(k_x - k_{\mathrm{pw},x})$ apparent in (16) turns into a $\mathrm{sinc}(\cdot)$. The truncated secondary source distribution therefore exhibits distinctive complex radiation properties.

The main lobe of the $\mathrm{sinc}(\cdot)$ function points into the propagation direction of the desired virtual plane wave. However, the reproduced sound field will not exhibit perfectly plane wave fronts but a certain curvature. The side lobes of the $\mathrm{sinc}(\cdot)$ function result in components in the reproduced sound field propagating into other directions than the desired virtual plane wave. Note that the side lobes exhibit alternating algebraic sign and that there are zeros between the lobes. Refer to Fig. 6. It depicts the sound field reproduced by a discrete truncated linear secondary monopole source distribution. The parameters were chosen such that no propagating aliasing artifacts arise. In Fig. 6(b), the directivity lobes due to truncation are clearly apparent. Refer to Section VIII for comments on the interaction of spatial sampling and truncation. It is also evident from Fig. 6 that the local propagation direction of the reproduced sound field strongly depends on the position of the receiver.

Real-world implementations of planar sound field reproduction systems are of course also truncated in z-dimension. Due to the separability of the Cartesian coordinate system, the truncation in the two dimensions can be treated independently. The procedure outlined above has to be applied also on the z-dimension.

Further analysis reveals that truncation artifacts can be interpreted as additional point sources located at the ends of the secondary source distribution [20].

Of course, other window functions can be applied some of which provide potential to shape truncation artifacts in order to make them perceptually less disturbing. This process is an established technique in WFS and is referred to as *tapering* [20]. Typically, windows with cosine-shaped shoulders are applied.

VIII. Further Aspects of Spatial Truncation and Discretization

In order to assess the properties of spatially truncated discrete secondary source distributions (which is in fact what we find in real-life), the findings derived in Sections VI and VII have to be combined. For convenience, we explicitly consider a discrete linear secondary source distribution which is truncated in x-dimension.

From (40) and (33) we can deduce that the reproduced sound field $\tilde{P}_{S,\mathrm{tr},|y|}(k_x, y, z, \omega)$ of a truncated discrete linear secondary source distribution is given in wavenumber domain by

$$\begin{aligned}\tilde{P}_{S,\mathrm{tr},|y|}(k_x, y, z, \omega) &= \frac{1}{2\pi} \underbrace{\left(\sum_{\eta=-\infty}^{\infty} \tilde{w}(k_x) *_{k_x} \tilde{D}(k_x - \frac{2\pi}{\Delta x}\eta, \omega) \right)}_{=\tilde{D}_{S,\mathrm{tr}}(k_x,\omega)} \\ &\quad \times \tilde{G}_{|y|}(k_x, y, z, \omega). \end{aligned} \tag{43}$$

For the interpretation of (40) we consider again the reproduction of a plane wave. Recall $\tilde{D}(k_x, \omega)$ given by (16). The spatial truncation does not only smear the energy of the desired components along the k_x but also the aliased components. It can thus happen that an aliasing contribution which is propagating for an infinite discrete secondary source distribution is partly smeared into the evanescent region $0 < |(\omega/c)| < k_x$ [refer to (52)]. This circumstance has already been indicated in [23]. Vice versa, an aliasing contribution which is evanescent for an infinite discrete secondary source distribution can partly be smeared into the propagating region where $0 < k_x < |(\omega/c)|$.

As a consequence, the interaction of spatial sampling and truncation results in a reduced reproducible spatial fine structure.

It has to be noted that the undesired evanescent components in the reproduced sound field exhibit an amplitude which is decaying rapidly with the distance to the secondary source array. They become negligible already at moderate distances [28].

Above derived findings are supported by results from [29] where it is shown that a bandlimited sound field has a limited complexity in a given spherical region. Thus, it can be resynthesized by a limited number of secondary sources. Inversely, a limited number of secondary sources (e.g., a truncated sampled array) is then only capable of reproducing a sound field with limited complexity.

Further investigation shows that the amplitude of the individual propagating aliasing components is strongly dependent on the location of the receiver [22], [23]. Typically, locations farther away from the secondary source distribution exhibit less spatial aliasing.

IX. Conclusion

A framework for the physical reproduction of plane-wave sound fields by continuous planar and linear secondary source arrangements was presented. For continuous planar secondary source distributions, the desired sound field is perfectly reproduced in one of the half-spaces defined by the secondary source distribution. The reproduced sound field in the other half-space is a byproduct whose properties are determined by the directivity of the secondary sources in that half-space. When omnidirectional secondary sources are employed, the reproduced sound field is symmetric with respect to the secondary source distribution.

The treatment of continuous linear secondary distributions revealed that the sound field can only be perfectly reproduced on an infinite line parallel to the secondary source distribution. When a virtual plane wave is intended to be reproduced, the reproduced sound field shows an amplitude decay of approximately 3 dB with every doubling of the distance and slight spectral deviations. Plane waves propagating parallel to the secondary source arrays cannot be recreated. This fact is mathematically reflected in a restricted validity of the involved transformations.

Spatial discretization of the secondary source distribution as occurring in real-world implementations leads to unavoidable evanescent components in the reproduced sound field when secondary monopole sources are assumed. In other words, a sampling theorem avoiding evanescent discretization artifacts does not exist. To the authors' awareness, investigations on the perception of evanescent sound fields like those apparent in the present study are not available in the literature. The perceptual consequences of these evanescent components in the reproduced sound field can therefore not be clarified in the scope of this paper.

For both planar as well as linear distributions and when secondary monopole sources are considered, additional propagating artifacts can arise when the spacing between adjacent secondary sources is too wide for a given temporal frequency to be reproduced. All propagating components reproduced by discrete linear secondary source distributions are unavoidably accompanied by an additional evanescent component. Existing practical implementations of sound field reproduction systems produce considerable spatial aliasing artifacts for temporal frequencies above a few thousand Hertz.

It was shown that the spatial truncation of the secondary source distribution also occurring in real-world implementations results in a complex directivity pattern exhibiting a main lobe, side lobes, and zeros. Aliasing artifacts which are propagating for infinite discrete secondary source distributions can become evanescent for finite distributions. Vice versa, aliasing artifacts which are evanescent for infinite discrete secondary source distribution can become propagative for finite distributions.

Since no ambiguities arose in the derivation of the driving functions, the solution can be assumed to be unique. This is in contrast to the situation when the receiver area is enclosed by the secondary source distribution. These setups suffer from non-uniqueness and ill-posedness [10], [30].

The comparison of the presented approach to the alternative formulation provided by the Rayleigh I integral showed that the two approaches are equivalent under equal assumptions. In the case of linear secondary source distributions, the Rayleigh formulation appears as an approximation of the presented approach whereby the former suffers from amplitude errors. The computational complexity is equally low for both formulations under equal assumptions.

APPENDIX A
DEFINITION OF THE FOURIER TRANSFORM

The temporal Fourier transform used in this paper is defined as

$$P(\mathbf{x},\omega) = \int_{-\infty}^{\infty} p(\mathbf{x},t)\, e^{-j\omega t}\, dt. \tag{44}$$

The spatial Fourier transform is defined as

$$\tilde{P}(k_x,y,z,\omega) = \int_{-\infty}^{\infty} P(\mathbf{x},\omega)\, e^{jk_x x}\, dx \tag{45}$$

exemplarily for the x-dimension.

The according inverse Fourier transforms are obtained by changing the algebraic sign in the exponent and normalizing with $(1/2\pi)$.

APPENDIX B
FOURIER TRANSFORMS OF A PLANE WAVE

A monochromatic plane wave with frequency ω_{pw} and unit amplitude propagating into the direction $(\theta_{\mathrm{pw}}, \phi_{\mathrm{pw}})$ is given by [3]

$$p(\mathbf{x},t) = e^{-j\mathbf{k}_{\mathrm{pw}}^T\mathbf{x}} \cdot e^{j\omega_{\mathrm{pw}}t}. \tag{46}$$

As discussed in Section II-A, the sound field described by (46) can not be perfectly recreated with the secondary source setups discussed in this paper. The reproduction is constricted to $p_{|y|}(\mathbf{x},t)$.

A Fourier transform of $p_{|y|}(\mathbf{x},t)$ with respect to t yields [19]

$$P_{|y|}(\mathbf{x},\omega) = e^{-j\mathbf{k}_{\mathrm{pw}}^T\mathbf{x}_{|y|}} \cdot 2\pi\delta(\omega-\omega_{\mathrm{pw}}). \tag{47}$$

A further Fourier transform with respect to x yields

$$\tilde{P}_{|y|}(k_x,y,z,\omega) = 2\pi\delta(k_x-k_{\mathrm{pw},x}) \times e^{-jk_{\mathrm{pw},y}|y|}\, e^{-jk_{\mathrm{pw},z}z} \times 2\pi\delta(\omega-\omega_{\mathrm{pw}}) \tag{48}$$

and finally with respect to z

$$\tilde{P}_{|y|}(k_x,y,k_z,\omega) = 4\pi^2\delta(k_x-k_{\mathrm{pw},x})\, e^{-jk_{\mathrm{pw},y}|y|} \times\delta(k_z-k_{\mathrm{pw},z}) \cdot 2\pi\delta(\omega-\omega_{\mathrm{pw}}) \tag{49}$$

whereby $\delta(\,\cdot\,)$ denotes the Dirac delta function [19].

APPENDIX C
FOURIER TRANSFORMS OF A POINT SOURCE

The spatial transfer function of an acoustic point source situated at the coordinate origin is given by [3]

$$g(\mathbf{x},t) = \frac{1}{4\pi}\frac{\delta(t-\frac{|\mathbf{x}|}{c})}{|\mathbf{x}|} \tag{50}$$

with $|\mathbf{x}| = \sqrt{x^2+y^2+z^2}$. The factor $(1/4\pi)$ was introduced for convenience to allow an interpretation of $g(\mathbf{x},t)$ as free-field Green's function [3] (refer to Section IV). We furthermore replace y^2 by $|y|^2$ in (50). This replacement is justified since $y^2 = |y|^2$. It will be of significance as discussed below.

The temporal Fourier transform of (50) is then

$$G_{|y|}(\mathbf{x},\omega) = \frac{1}{4\pi}\frac{e^{-j\frac{\omega}{c}|\mathbf{x}_{|y|}|}}{|\mathbf{x}_{|y|}|}. \tag{51}$$

The Fourier transform with respect to x is calculated by applying Euler's formula [31] and using [32, (3.876-1) and (3.876-2)] and [33, p. 1323]. It is given by (52) shown at the bottom of the page. $H_0^{(2)}(\,\cdot\,)$ denotes the zeroth-order Hankel function of second kind, $K_0(\,\cdot\,)$ the zeroth-order modified Bessel function of second kind [3]. A further Fourier transform with respect to z is yielded using [32, (6.677-3), (6.677-4), and (6.677-5)]. It is given by (53) shown at the top of the next page. By having replaced y^2 with $|y|^2$ as discussed above, we ensured the validity of (53) for all possible values of y [32].

REFERENCES

[1] M. Gerzon, "With-heigth sound reproduction," *JAES*, vol. 21, pp. 2–10, 1973.

[2] A. Berkhout, D. de Vries, and P. Vogel, "Acoustic control by wave field synthesis," *JASA*, vol. 93, no. 5, pp. 2764–2778, May 1993.

[3] E. G. Williams, *Fourier Acoustics: Sound Radiation and Nearfield Acoustic Holography*. London: Academic, 1999.

[4] D. Ward and T. Abhayapala, "Reproduction of a plane-wave sound field using an array of loudspeakers," *IEEE Trans. Speech Audio Process.*, vol. 9, no. 6, pp. 697–707, Sep. 2001.

[5] J. Daniel, "Représentation de champs acoustiques, application à la transmission et à la reproduction de scènes sonores complexes dans un contexte multimédia," Ph.D. dissertation, Univ. Paris 6, Paris, France, 2001.

[6] M. Poletti, "Three-dimensional surround sound systems based on spherical harmonics," *JAES*, vol. 53, no. 11, pp. 1004–1025, Nov. 2005.

$$\tilde{G}_{|y|}(k_x,y,z,\omega) = \begin{cases} -\frac{j}{4}H_0^{(2)}\left(\sqrt{\left(\frac{\omega}{c}\right)^2-{k_x}^2}\sqrt{|y|^2+z^2}\right), & \text{for } |k_x| < \left|\frac{\omega}{c}\right| \\ \frac{1}{2\pi}K_0\left(\sqrt{{k_x}^2-\left(\frac{\omega}{c}\right)^2}\sqrt{|y|^2+z^2}\right), & \text{for } \left|\frac{\omega}{c}\right| < |k_x| \end{cases} \tag{52}$$

$$\tilde{G}_{|y|}(k_x, y, k_z, \omega) = \begin{cases} -\frac{j}{2}\frac{e^{-j\sqrt{\left(\frac{\omega}{c}\right)^2 - k_x^2 - k_z^2}\cdot|y|}}{\sqrt{\left(\frac{\omega}{c}\right)^2 - k_x^2 - k_z^2}}, & \text{for } 0 \le \sqrt{k_x^2 + k_z^2} < \left|\frac{\omega}{c}\right| \\ \frac{1}{2}\frac{e^{-\sqrt{k_x^2 + k_z^2 - \left(\frac{\omega}{c}\right)^2}\cdot|y|}}{\sqrt{k_x^2 + k_z^2 - \left(\frac{\omega}{c}\right)^2}}, & \text{for } 0 < \left|\frac{\omega}{c}\right| < \sqrt{k_x^2 + k_z^2} \end{cases} \tag{53}$$

[7] J. Hannemann and K. Donohue, "Virtual sound source rendering using a multipole-expansion and method-of-moments approach," *JAES*, vol. 56, no. 6, pp. 473–481, Jun. 2008.

[8] J. Ahrens and S. Spors, "An analytical approach to sound field reproduction using circular and spherical loudspeaker distributions," *Acta Acust. Utd. With Acust.*, vol. 94, no. 6, pp. 988–999, Nov./Dec. 2008.

[9] Y. J. Wu and T. D. Abhayapala, "Theory and design of soundfield reproduction using continuous loudspeaker concept," *IEEE Trans. Audio, Speech, Lang. Process.*, vol. 17, no. 1, pp. 107–116, Jan. 2009.

[10] F. Fazi, P. Nelson, J. Christensen, and J. Seo, "Surround system based on three dimensional sound field reconstruction," in *Proc. 125th Conv. AES*, San Francisco, CA, Oct. 2–5, 2008.

[11] O. Kirkeby and P. Nelson, "Reproduction of plane wave sound fields," *JASA*, vol. 94, no. 5, pp. 2992–3000, Nov. 1993.

[12] S. Spors, R. Rabenstein, and J. Ahrens, "The theory of wave field synthesis revisited," in *Proc. 124th Conv. AES*, Amsterdam, The Netherlands, May 17–20, 2008.

[13] D. D. Vries, "Sound reinforcement by wavefield synthesis: Adaptation of the synthesis operator to the loudspeaker directivity characteristics," *JAES*, vol. 44, no. 12, pp. 1120–1131, Dec. 1996.

[14] O. Kirkeby, P. Nelson, H. Hamada, and F. Orduna-Bustamante, "Fast deconvolution of multichannel systems using regularization," *IEEE Trans. Speech Audio Process.*, vol. 6, no. 2, pp. 189–195, Mar. 1998.

[15] J. J. Lopez, A. Gonzalez, and L. Fuster, "Room compensation in wave field synthesis by means of multichannel inversion," in *Proc. IEEE Workshop Appl. Signal Process. Audio Acoust. (WASPAA)*, New Paltz, NY, Oct. 2005.

[16] E. Corteel, "Equalization in an extended area using multichannel inversion and wave field synthesis," *JAES*, vol. 54, no. 12, pp. 1140–1161, Dec. 2006.

[17] S. Spors, H. Buchner, R. Rabenstein, and W. Herbordt, "Active listening room compensation for massive multichannel sound reproduction systems using wave-domain adaptive filtering," *JASA*, vol. 122, no. 1, pp. 354–369, Jul. 2007.

[18] J. Ahrens and S. Spors, "Reproduction of a plane-wave sound field using planar and linear arrays of loudspeakers," in *Proc. IEEE Int. Symp. Comm., Control, Signal Process. (ISCCSP)*, Malta, Mar. 12th–14th, 2008.

[19] B. Girod, R. Rabenstein, and A. Stenger, *Signals and Systems*. New York: Wiley, 2001.

[20] E. Verheijen, "Sound reproduction by wave field synthesis," Ph.D. dissertation, Delft Univ. of Technol., Delft, The Netherlands, 1997.

[21] E. W. Start, "Direct sound enhancement by wave field synthesis," Ph.D. dissertation, Delft Univ. of Technol., Delft, The Netherlands, 1997.

[22] S. Spors, "Spatial aliasing artifacts produced by linear loudspeaker arrays used for wave field synthesis," in *Proc. IEEE Int. Symp. Commun., Control, Signal Process.*, Marrakech, Morocco, Mar. 2006.

[23] B. Pueo, J. J. Lopez, J. Escolano, and S. Bleda, "Analysis of multiactuator panels in space-time wavenumber domain," *JAES*, vol. 55, no. 12, pp. 1092–1106, Dec. 2007.

[24] H. Wittek, "Perceptual differences between wavefield synthesis and stereophony," Ph.D. dissertation, Univ. of Surrey, Guildford, U.K., 2007.

[25] W. de Brujin, "Application of wave field synthesis in videoconferencing," Ph.D. dissertation, Delft Univ. of Technol., Delft, The Netherlands, 2004.

[26] J. Sanson, E. Corteel, and O. Warusfel, "Objective and subjective analysis of localization accuracy in wave field synthesis," in *124th Conv. of the AES*, Amsterdam, The Netherlands, May 17–20, 2008.

[27] S. Spors, "Investigation of spatial aliasing artifacts of wave field synthesis in the temporal domain," in *Proc. 34rd German Annu. Conf. Acoust. (DAGA)*, Dresden, Germany, Mar. 2008.

[28] S. Spors and J. Ahrens, "Analysis of near-field effects of wave field synthesis using linear loudspeaker arrays," in *Proc. 30th Int. Conf. Audio Eng. Soc. (AES)*, Mar. 2007.

[29] R. Kennedy, P. Sadeghi, T. Abhayapala, and H. Jones, "Intrinsic limits of dimensionality and richness in random multipath fields," *IEEE Trans. Signal Process.*, vol. 55, no. 6, pp. 2542–2556, Jun. 2007.

[30] S. Spors and J. Ahrens, "Towards a theory for arbitrarily shaped sound field reproduction systems," *JASA*, vol. 123, no. 5, p. 3930, 2008.

[31] E. Weisstein, "Euler Formula. MathWorld—A Wolfram Web Resource," [Online]. Available: http://mathworld.wolfram.com/EulerFormula.html Retrieved June 09

[32] I. Gradshteyn and I. Ryzhik, *Table of Integrals, Series, and Products*. San Diego, CA: Academic, 2000.

[33] P. M. Morse and H. Feshbach, *Methods of Theoretical Physics*. Minneapolis, MN: Feshbach, 1953.

Jens Ahrens received the Dipl.-Ing. degree with distinction in electrical engineering/sound engineering from Graz University of Technology and University of Music and Dramatic Arts Graz, Graz, Austria, in 2005. He is currently working towards the Dr.-Ing. degree in electrical engineering at Deutsche Telekom Laboratories, Technische Universität Berlin, Berlin, Germany.

His current areas of interest include sound reproduction using massive multichannel reproduction systems like wave field synthesis and higher-order Ambisonics and sound field analysis using microphone arrays.

Sascha Spors received the Dipl.-Ing. degree in electrical engineering and the Dr.-Ing. degree from the University of Erlangen-Nuremberg, Erlangen, Germany, in 2000 and 2006, respectively.

He is a Senior Research Scientist at Deutsche Telekom Laboratories, Technische Universität Berlin, Berlin, Germany. From 2001 to 2005, he was a Member of the Research Staff at the Chair of Multimedia Communications and Signal Processing, University of Erlangen-Nuremberg. He holds several patents, has authored or coauthored five book chapters, and more than 90 papers in journals and conference proceedings. His current areas of interest include sound reproduction using massive multichannel reproduction systems like wave field synthesis and higher-order Ambisonics, sound field analysis using microphone arrays and efficient multichannel algorithms for adaptive digital filtering.